Financial analytics of inverse BTC options in a stochastic volatility world[*]

Huei-Wen Teng[†]

Wolfgang Karl Härdle[‡]

October 5, 2022

Abstract

Bitcoin (BTC) has attracted a plethora of investors and professional traders and becomes an almost inevitable asset class in today's financial markets. Deribit, the largest exchange for crypto options, offers European-typed inverse options, which target to BTC in USD but have payoff denominated in BTC. However, analytical insights to inverse options remain scarce. The dynamics of the underlying BTC is well described by a stochastic volatility model but in pricing inverse options one meets numerical difficulties in calibration and hedging. Financial analytics for the practically useful stochastic volatility with correlated jumps model is provided and comparison with simpler nested models both in in-sample and out-of-sample pricing is given. A dynamic Delta hedging exercise yields that - surprisingly - the portfolio of nested models gives almost identical hedging errors.

Keywords: cryptocurrency, crypto options, stochastic volatility models, correlated jumps, simulation, Delta hedge, CRIX, crypto index.

JEL Codes: G13, C15, C58, E37

1 Introduction

Bitcoin (BTC) was the first open-source distributed cryptocurrency (CC) after the white paper by **?**. Other CC's followed and together now they represent a market cap more than that of the top twenty stocks worldwide in Q2 2022. Financial institutions have therefore constructed tailor-made products for investors involing CCs for portfolio diversification (**?**). BTC has become therefore an inevitable asset requiring analytical insight into its derivatives market. As the largest exchange for crypto options, Deribit offers the "inverse option", where BTC denominated in USD is the underlying asset, but the payoff is denominated in BTC. As a consequence, this option type allows professional traders to avoid exchanging frequently between fiat money and CC.

An intriguing feature of this inverse option is its non-linear payoff. Let us look at two examples. Suppose that the current BTC is traded at 20,000 USD and focus on an at-the-money (ATM) option with strike 20,0000 USD. If the BTC raises to 40,000 at maturity, the payoff for the inverse BTC call option with strike 20,000 USD is worth simply 0.5 BTC. On the contrary, if the BTC drops to 5,000 BTC at maturity, the payoff for the inverse BTC put option with strike 20,000 USD is valued at 3 BTCs. These two examples display this striking asymmetry of the payoff.

Earlier work include **?**, **?** focussing e.g. on various GARCH models. **?** works with jump-diffusion models, and **?** apply mixed jump-diffusion process. **?** compare the Black-Scholes, Laplace model, five variance gamma-related models, and the Heston model for BTC prices. **?** includes market attention as an exogenous factor as an extension to the geometric Brownian motion. **?** consider stochastic volatility with correlated jumps models. These papers estimate dynamics using BTC prices, then produce prices for the plain vanilla options. But, we calibrate complex models using real options data directly.

With simulated option prices of the plain vanilla type, **?** simulate complex dynamics for CC to study hedging performance. An increasing number of studies start to investigate crypto options with real data, but they also apply the vanilla option. For example, **?** combines a multiple input LSTM-based model with the Black-Scholes model; **?** calculate implied volatility under the pricing formulae for vanilla options; **?** compare the Heston-

2

Nandi GARCH (1,1) asymmetric multiple volatility-regime model with Black-Scholes model.

? is the first paper highlighting that the inverse option type is dominating (rather than the vanilla option) in the CC market. Considering inverse options under the Black-Scholes model, **?** contrast IV curves of tick-level Deribit option price data with those of S&P 500 options, and **?** analyse robust dynamic delta hedging of BTC options. However, these studies are restricted to the Black-Scholes model. Because stylized features in the dynamics of BTC include SV and jumps from numerical empirical studies, this paper aims at understanding whether a more complex dynamics helps to price and hedge crypto options.

A first difficulty in model calibration is the lack of closed-form pricing formulae for a complex dynamics. Even for the relatively simple Heston's Stochastic Volatility (SV) model, calibration using plain vanilla options remains a challenge (**??**). Dynamics of CCs have been documented to be extremely volatile and to contain frequent jumps (**???**). To incorporate these features, this paper aims at investigating if the practically useful SV with correlated jumps outperforms simpler model in pricing and hedging for the inverse option. Although Monte Carlo simulation can be used to price the inverse option, it is notoriously known for its slow convergence. Worse, its variability in each Monte Carlo simulation deteriorates the iteration in the optimization process. To overcome this difficulty in model calibration, we first provide a feasible simulation scheme for model calibration using common random variables (**?**).

Once calibrated, we calculate the Greeks for implementing hedging routines (**?**). Greeks are price sensitivities of option price with respect to certain parameters and are critical measures for risk management in derivatives market. Among Greeks, the Delta Δ is the first-order partial differentiation of option price with respect to the initial price of the underlying asset and is used to hedge the change of the underlying asset. The calculation of Greeks is not straightforward, particularly when there exists no closed-form pricing formulae for a specific option with complex dynamics (**?**). As a second numerical contribution of this paper, we apply the parameter derivative in **?** to provide an unbiased

Delta formula under various stochastic volatility models, which coincides with the Delta formula in **?** for the Black-Scholes case. The Delta formula allows traders dynamic hedging for the described setting and their helps in creating stable portfolio with predefined risk structure.

The rest of this paper is organized as follows. Section 2 explores the inverse options based on data of the Blockchain-Research-Center.com and demonstrates a puzzle for implied volatility slippery. Section 3 calibrates and investigates implied parameters of the stochastic volatility with correlated jumps model and its nested models. It also compares in-sample and out-of-sample pricing errors. Section 4 provides the Delta formula and implements dynamic Delta hedging. The last section concludes. All code for this paper is available on Q quantlet.com. A presentation video of this paper is on Q quantinar.com.

2 Inverse options

In the following, Section 2.1 contrasts the payoff function for vanilla options and inverse options, Section 2.2 explores the data, and Section 2.3 presents the slippery of implied volatility for inverse options.

2.1 The payoff function

Let K be the strike price, and T be the time to maturity in days. We use an indicator $\omega = 1$ and $\omega = -1$ for a call and put option, respectively. In addition, let r denote the discount rate, and y denote the dividend yield. Let S_t denote the BTC price denominated in USD at time t. Recall the European plain vanilla option with payoff,

$$\wp_{vanilla}(\omega, K, T) = \max\left\{\omega(S_T - K), 0\right\}, \ \omega = \pm 1. \tag{1}$$

Vanilla options have piecewise linear payoff functions, which guarantees the put-call parity.

A distinct feature of the inverse option is that its strike price corresponds to the value of a BTC denominated in USD, but the payoff is converted back to BTC. Let $S_t^{-1} = \frac{1}{S_t}$

denote the inverse of the price S_t. The inverse option has therefore the payoff

$$\wp_{inverse}(\omega, T, K) = S_T^{-1} \max \left\{ \omega(S_T - K), 0 \right\}, \ \omega = \pm 1. \tag{2}$$

In contrast to the payoff (1), inverse options have piecewise nonlinear payoff functions, and thus the standard put-call parity does not hold and hence also the implied volatility of put and call are different.

Figure 1 depicts the payoff function against S_T for vanilla and inverse BTC call and put options. Suppose the strike price is K USD. Recall that the payoff for a vanilla option is denominated in dollars, but the payoff for an inverse option is denominated in BTC. Although vanilla options may have unlimited positive payoff, this is not the case for inverse options. Specifically, the inverse BTC call option has a payoff capped with one BTC, but the inverse put option has unlimited positive payoff. This indicates that inverse BTC call options should be priced less than one BTC, otherwise, an arbitrage opportunity will exist. However, an inverse BTC put option could be worth more than one BTC in the real market. For example, an inverse BTC put option has a payoff of five BTCs if BTC drops to one-fifth of the strike price at maturity. As indicated already, all numerical examples can be replayed by checking the **Q** Quantlet.com link.
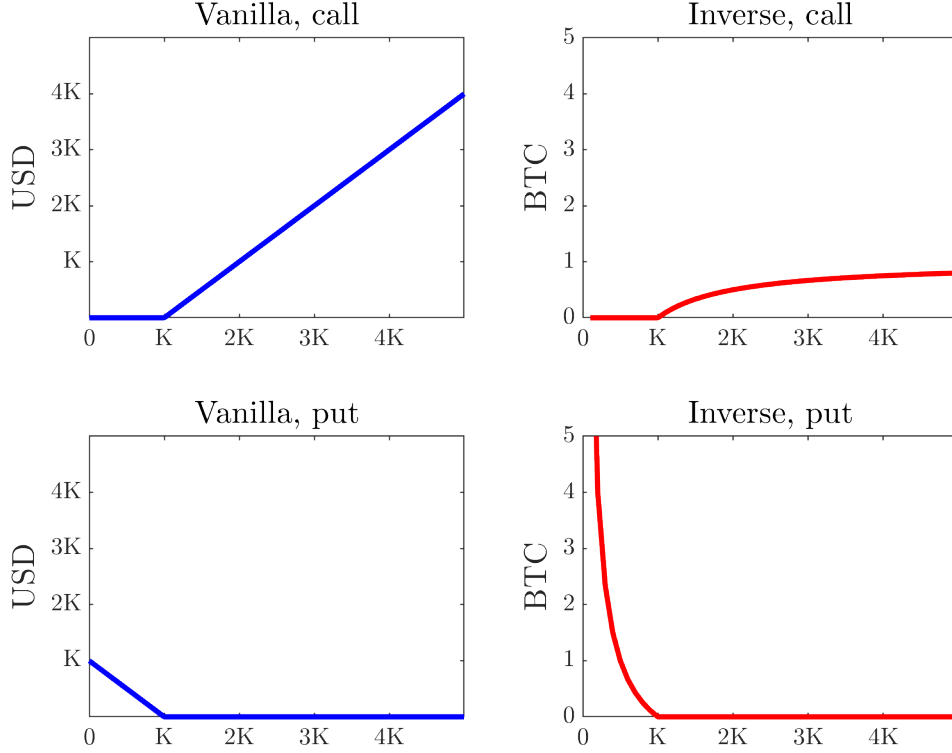
Figure 1: **Payoff functions of vanilla and inverse options**. This figure contrasts payoff against S_T between vanilla and inverse options. Suppose the strike price is K USD. The first and second columns depict payoff for vanilla and inverse options, respectively. The first and second rows depict payoff for call and put options, respectively. It is shown that vanilla options have piecewise linear functions, whereas inverse options have nonlinear payoff functions. In addition, the inverse call option has payoff capped with one BTC, but the inverse put option has unlimited positive payoff. Q Deribit_inverse_BTC_options

2.2 Data

In this research, we collect Deribit intraday transaction data for inverse options through Blockchain-Research-Center.com during December 1, 2021 to February 28, 2022. The dataset includes 736,563 observations, a total of 90 trading days. As of this writing (September 2, 2022), among the total BTC options with open interest at 243.60K BTC, Deribit takes a dominating proportion at 88% (215.90K BTC), followed by CME at 8% (16.44K BTC), and Okex at 3% (8.44K BTC). Table 5 in the Appendix summarize columns and explanations for each column of the data. The intraday transaction data includes information such as timestamps, BTC prices in USD, implied volatility, types, strikes, and maturities of inverse options. This information allows us to obtain a full picture of the BTC options market.

Figure 2 sketches the time series of daily accumulative numbers of trades and daily accumulative volume from the intraday transaction for inverse options. One sees that both daily numbers of trades and volume are stable for the defined time period. The average daily number of trades is 8,184, and the average volume is 21,155.
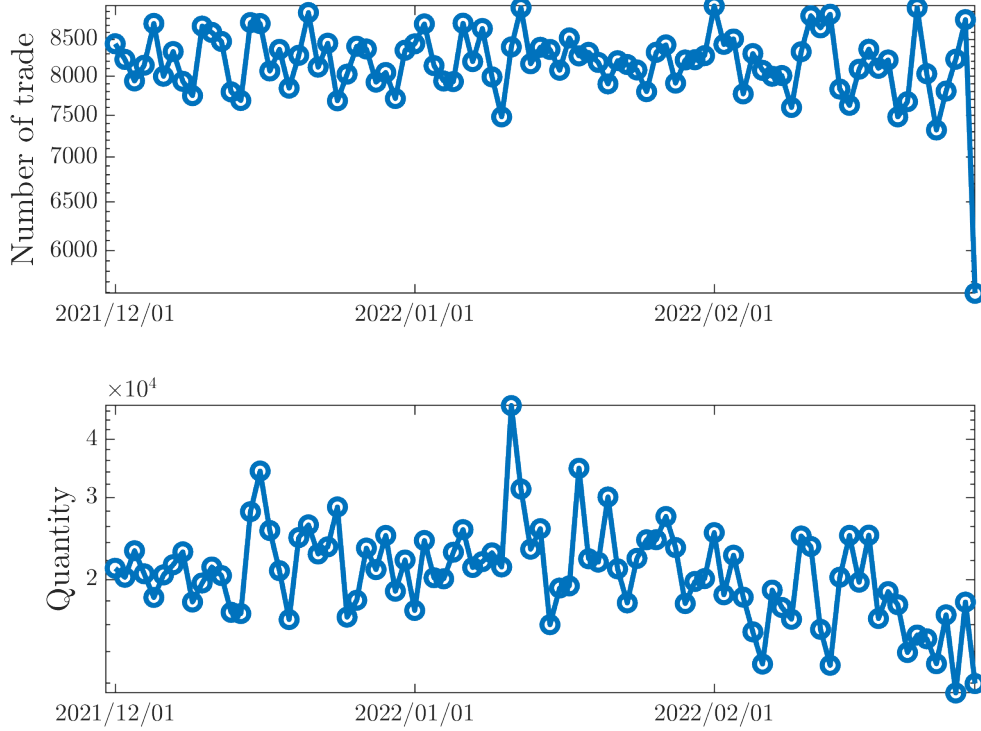

Figure 2: **Daily accumulated trades and quantities**. For intraday transaction on inverse options, the upper panel provides time series plot for daily accumulative number of trades, and the lower panel provides time series plot for daily accumulated quantities. The study period spans from December 1, 2021 to February 28, 2022. Deribit_inverse_BTC_options

Figure 3 depicts strike prices of intraday transaction for inverse BTC call and put options during the study period, and overlays the intraday BTC prices in a black bold line. First, it may be noted that out-of-the-money (OTM) options are more frequently traded compared with in-the-money (ITM) options: Inverse BTC call options are more frequently traded at strike prices above current BTC prices, whereas inverse BTC put options are more frequently traded at strike prices below current BTC prices. Second, one discovers that the range of strike price is substantially larger than the range for classical option market. The average BTC is 43,874.72 USD, but the minimum and maximum strike prices are 12,000 USD and 400,000 for the inverse option, respectively.

7
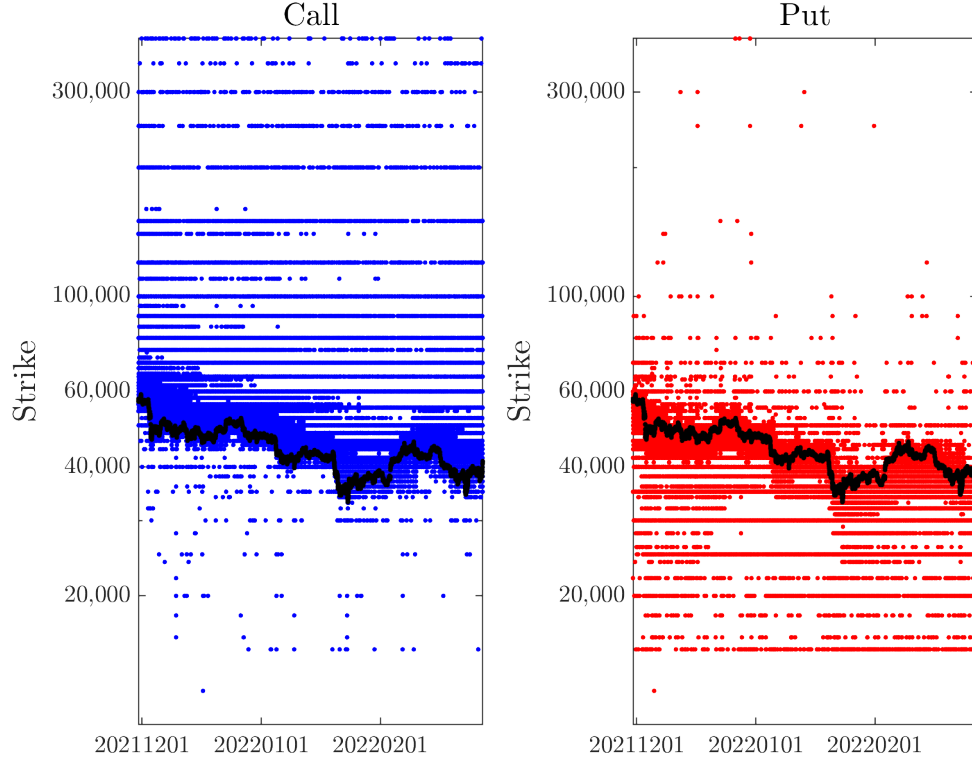
Figure 3: **Visualizing strike prices for intraday transaction of inverse options**. The left panel and right panel depict strike prices for intraday transaction of inverse BTC call and put options, respectively. The BTC prices are depicted in a black bold line. The study period spans from December 1, 2021 to February 28, 2022.
🔍 Deribit_inverse_BTC_options

Figure 4 depicts a three-dimensional scatter plot for prices of inverse options traded on January 1, 2022. It is clear that inverse options are more frequently traded with short-term maturity and at a wide range of moneyness. In addition, excluding the highest 0.1% prices of BTC inverse options, all options have prices less than 0.2 BTC.
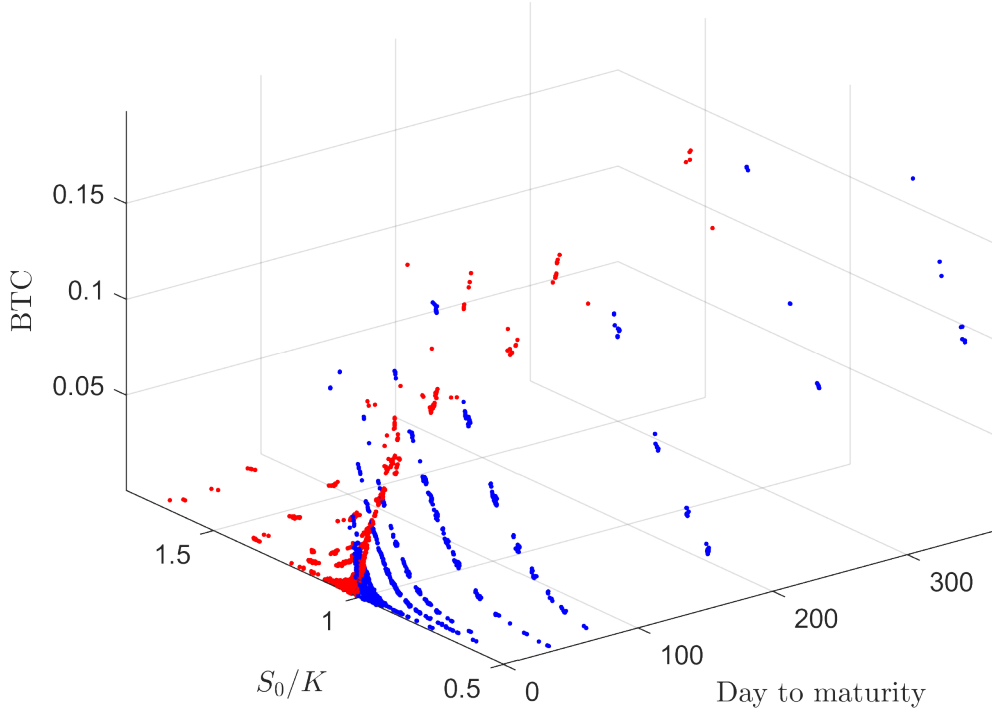
Figure 4: **Visualizing prices of inverse options**. This figure depicts a 3-D scatter plot for prices of inverse options traded on January 18, 2022. Call and put options are depicted in blue and red colors, respectively. We remove the highest 0.1% prices of BTC inverse options to have a better demonstration. 🔍 Deribit_inverse_BTC_options

Table 1 provides percentiles of time to maturity (T), moneyness (K/S_0), and prices for intraday transaction. About 50% of the options are short-term: Inverse call and put options have a median of time maturity 9 and 7, respectively. Second, more than 90% of the options are traded OTM. However, 5% are traded at extremely high or low strike prices: The 5th percentile of moneyness for call options is 0.51, and the 95th percentile of moneyness for put options is 1.55.

Table 1: **Distributions of option characteristics**. This table reports percentiles for the time to maturity (T), moneyness (S_0/K), and prices (p) of inverse BTC call and put options. Here, Q_k denotes the k-th percentile. The study period spans from December 1, 2021 to February 28, 2022. **Q** Deribit_inverse_BTC_options

	T		S_0/K		p	
Percentile	Call	Put	Call	Put	Call	Put
Min	0	0	0.09	0.12	0.0001	0.0002
Q_1	0	0	0.27	0.85	0.0005	0.0005
Q_5	1	0	0.51	0.96	0.0005	0.0010
Q_{10}	1	1	0.64	0.99	0.0010	0.0015
Q_{20}	1	1	0.78	1.00	0.0030	0.0035
Q_{30}	2	2	0.86	1.02	0.0055	0.0055
Q_{40}	6	4	0.91	1.03	0.0080	0.0090
Q_{50}	9	7	0.94	1.05	0.0115	0.0130
Q_{60}	15	12	0.96	1.08	0.0170	0.0190
Q_{70}	22	18	0.98	1.12	0.0250	0.0280
Q_{80}	42	30	0.99	1.21	0.0380	0.0435
Q_{90}	84	64	1.00	1.38	0.0630	0.0740
Q_{95}	149	105	1.02	1.55	0.0954	0.1095
Q_{99}	291	259	1.06	2.11	0.1750	0.2275
$Q_{99.9}$	355	347	1.34	2.91	0.3260	0.6375
$Q_{99.99}$	363	364	2.63	3.38	0.6255	4.2101
Max	365	365	3.90	4.04	0.7465	7.3356

Since, as noted above, the options are traded on a much wider range of moneyness than for standard options, we define maturity-moneyness categories in Table 2. We report the proportions of traded options in each maturity-moneyness category. Call options represent 55.6% of the trades, and 82.3% of the options are OTM. For the rest of this

section, we summarize the basic empirical findings.

Table 2: **Maturity-moneyness categories**. This table defines nine maturity-moneyness categories. For maturity, short-term, mid-term, and long-term options are defined according to time to maturity (T). Definitions for OTM, ITM, and deep ITM options are according to the moneyness (S_0/K). This table also reports proportions (%) of trades for inverse options at each maturity-moneyness category.
⚲ `Deribit_inverse_BTC_options`

Inverse BTC call option	Deep OTM	OTM	ITM	
	$\frac{S_0}{K} \leq 0.86$	$0.86 < \frac{S_0}{K} \leq 1$	$1 < \frac{S_0}{K}$	Sum
Short-term: $T \leq 5$	0.3%	16.3%	3.7%	20.3%
Mid-term: $5 < T \leq 28$	6.0%	12.9%	1.8%	20.7%
Long-term: $28 < T$	10.9%	3.0%	0.7%	14.6%
Sum	17.2%	32.2%	6.2%	55.6%
Inverse BTC put option	ITM	OTM	Deep OTM	
	$\frac{S_0}{K} \leq 1$	$1 < \frac{S_0}{K} \leq 1.12$	$1.12 < \frac{S_0}{K}$	Sum
Short-term: $T \leq 5$	3.5%	13.5%	1.1%	18.1%
Mid-term: $5 < T \leq 28$	2.5%	7.8%	6.4%	16.7%
Long-term: $28 < T$	1.3%	2.3%	6.0%	19.6%
Sum	7.3%	23.6%	13.5%	44.4%

Table 3 reports average prices and standard deviations (in parenthesis) for call and put options at each maturity-moneyness category. Average prices for call options are less than one BTC at all maturity-moneyness categories. In addition, it is consistent with intuitions that inverse options are more expensive for longer-term and deeper ITM, for both call and put options.

Table 3: **Average prices in BTC and standard deviations of inverse options**. This table reports average prices and standard deviations (in parenthesis) for options at each maturity-moneyness category. ⊙ Deribit_inverse_BTC_options

Inverse BTC call option	Deep OTM $\frac{S_0}{K} \leq 0.86$	OTM $0.86 < \frac{S_0}{K} \leq 1$	ITM $1 < \frac{S_0}{K}$
Short-term: $T \leq 5$	0.0006	0.0054	0.0232
	(0.0003)	(0.0049)	(0.0190)
Mid-term: $5 < T \leq 28$	0.0059	0.0224	0.0683
	(0.0059)	(0.0154)	(0.0468)
Long-term: $28 < T$	0.0358	0.0865	0.1614
	(0.0391)	(0.0477)	(0.0946)
Inverse BTC put option	ITM $\frac{S_0}{K} \leq 1$	OTM $1 < \frac{S_0}{K} \leq 1.12$	Deep OTM $1.12 < \frac{S_0}{K}$
Short-term: $T \leq 5$	0.0172	0.0041	0.0013
	(0.0558)	(0.0052)	(0.0011)
Mid-term: $5 < T \leq 28$	0.0695	0.0234	0.0071
	(0.0815)	(0.0145)	(0.0062)
Long-term: $28 < T$	0.1884	0.0816	0.0342
	(0.3674)	(0.0373)	(0.0289)

Figure 5 provides histograms of prices (p), days to maturity (T), and moneyness ($\frac{S_0}{K}$) for inverse put options with prices larger than one. It is fascinating that a put option is likely to be worthy more than one BTC. In fact, there are 130 put options, or about 0.04% of put options that have prices larger than one BTC. If we see the distribution of these extremely high priced put options, they are mostly long-term and deep ITM (with moneyness between 0.5 to 0.1). The data indicates that investors believe that there is a chance that the BTC price drops to one-half or one-tenth of current BTC price, respectively.
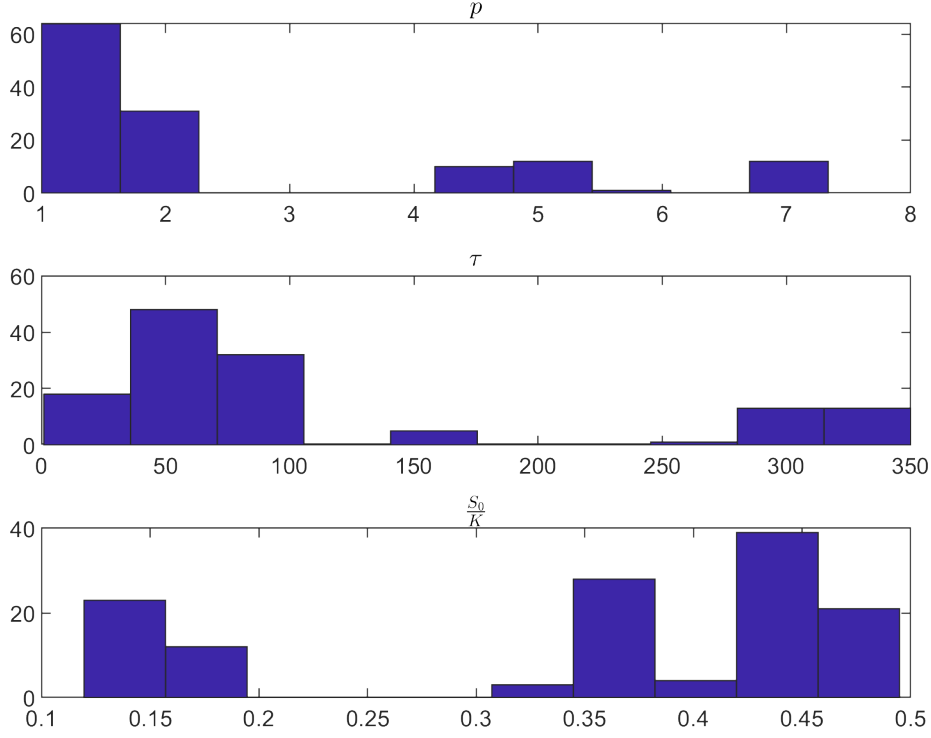
Figure 5: **Extremely high prices of inverse BTC put options**. This figure provides histograms of prices (p), days to maturity (T), and moneyness $(\frac{S_0}{K})$ for inverse put options with prices larger than one. The study period spans from December 1, 2021 to February 28, 2022. 🔍 `Deribit_inverse_BTC_options`

2.3 Slippery of implied volatility

Suppose for a moment the dynamics of S follows a geometric Brownian motion (GBM) with volatility σ. **?** provide pricing formulae

$$m_{BS}(\sigma; \omega, T, K) = \omega \left\{ e^{-rT} \Phi(\omega d_2) - e^{(y-r+\sigma^2)T} S_0^{-1} K \Phi(\omega d_3) \right\},\qquad (3)$$

where

$$d_1 = \frac{\frac{S_0}{K} + (r - y + \frac{1}{2}\sigma^2)T}{\sigma\sqrt{T}}, \ d_2 = d_1 - \sigma\sqrt{T}, \ d_3 = d_2 - \sigma\sqrt{T}.$$

In practice, the implied volatility (IV) $\sigma_{BS} \overset{\text{def}}{=} \sigma_{BS}(\omega, T, K)$ is calibrated by solving

$$m_{BS}(\sigma_{BS}; \omega, T, K) = p(\omega, T, K).\qquad (4)$$

In the introduced quantlet links, `fsolve` (a Matlab function) is used to calculate σ_{BS}. Discrepancies between iv communicated from Deribit and σ_{BS} are displayed in Figure 6. However, one discovers substantial differences and a discernible curvature.
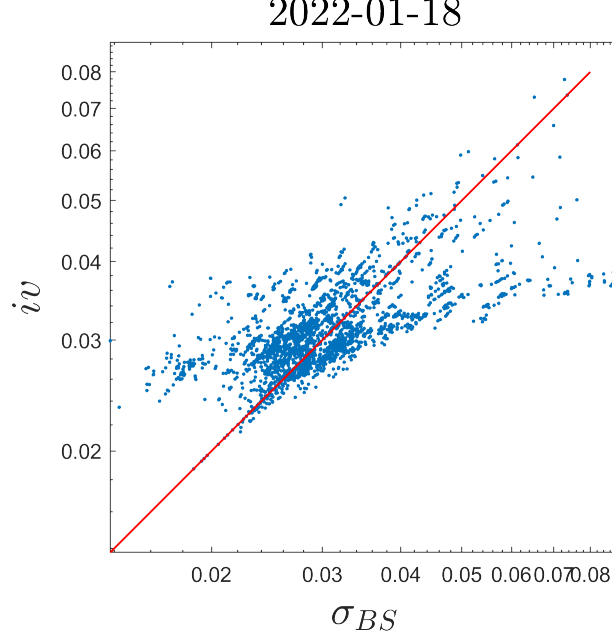

Figure 6: **Discrepancies between iv and σ_{BS}.** This figure plots iv against σ_{BS}, which solves (4) from our algorithm, and overlays a 45 degree line in red color. The data is on January 18, 2022. Similar patterns can be found in other dates. **Q** `Deribit_inverse_BTC_options`

To check which IV is representing the risk structure of this data analysis, plug iv and σ_{BS} in (3):

$$m_{BS}(iv) \overset{\text{def}}{=} m_{BS}(iv; \omega, T, K),$$

$$m_{BS}(\sigma_{BS}) \overset{\text{def}}{=} m_{BS}(\sigma_{BS}; \omega, T, K).$$

Figure 7 investigates if iv and σ_{BS} can successfully reproduce the prices, in the upper and lower panels, respectively. One sees that a large proportion of $m_{BS}(\sigma_{BS})$ lays on the 45 degree line. This indicates that σ_{BS} is able to reproduce the market price of inverse options. However, still a small proportion of $m_{BS}(\sigma_{BS})$ is in the upper part of the 45 degree line. This hints the inappropriateness of BS model in practice. On the other hand, $m_{BS}(iv)$ deviates from price p. Thus, the reported iv indeed posts a pricing puzzle for inverse options.
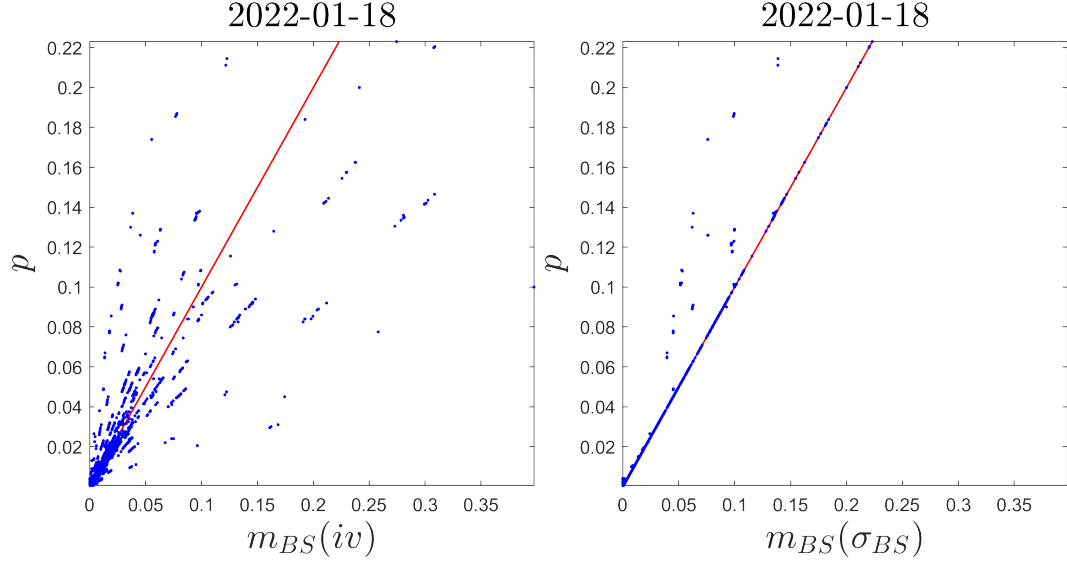
Figure 7: **Pricing inverse options using the BS formulae through** iv **and** σ_{BS}. The left and right panels plot market prices of inverse option (p) against model prices $m_{BS}(iv)$ and $m_{BS}(\sigma_{BS})$, respectively, using the intraday transaction of inverse options on January 18, 2022. Both panels overlay a 45 degree line in red color. Deribit_inverse_BTC_options

Figure 8 visualizes iv and σ_{BS} calibrated on January 18, 2022, in a 3-D scatter plot. These two implied volatilities have discernibly different patterns. Given a time to maturity, σ_{BS} appears to expose higher curvature across moneyness, yet iv is relatively flat. This higher curvature pattern in comparison with iv is a visible fact also on other trading days.
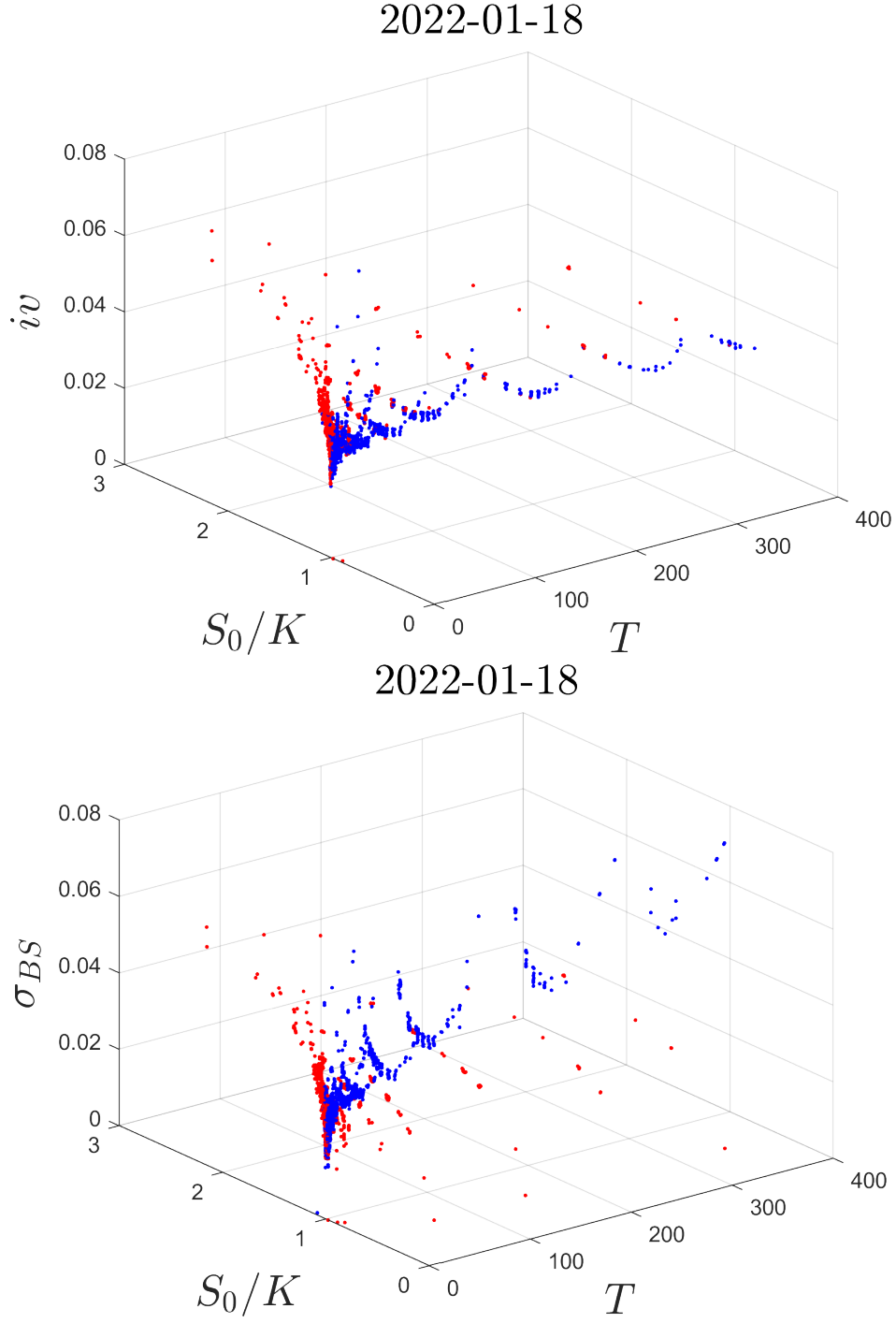
2022-01-18

2022-01-18

Figure 8: **Implied volatility** iv **and** σ_{BS}. The upper and lower panels depict scatter plots for iv and σ_{BS}, respectively. Data is on January 18, 2022. σ_{BS} is more skewed.

Deribit_inverse_BTC_options

3 Pricing inverse options

To start, Section 3.1 introduces the stochastic volatility with correlated jumps model and its nested ones. Then, Section 3.2 proposes a feasible simulation scheme in the stochastic optimisation for model calibration. Section 3.3 summarizes implied parameters and compares in-sample and out-of-sample pricing errors among different models.

3.1 The stochastic volatility with correlated jumps model

We turn now to pricing and explaining a stochastic volatility with correlated jumps (SVCJ) model, advocated as appropriate stochastic dynamics by **?**. The SVCJ model reads as:

$$\frac{dS_t}{S_t} = rdt + \sqrt{V_t}dW_t^s + Z_t^y dN_t \tag{5}$$

$$dV_t = \kappa(\theta - V_t)dt + \sigma_v\sqrt{V_t}dW_t^v + Z_t^v dN_t \tag{6}$$

$$Cov(dW_t^s, dW_t^v) = \rho dt \tag{7}$$

$$P(dN_t = 1) = \lambda dt \tag{8}$$

$$Z_t^y | Z_t^v \sim N(\mu_y + \rho_j Z_t^v, \sigma_y^2), \tag{9}$$

$$Z_t^v \sim Exp(\mu_v), \tag{10}$$

Since we are looking at short-term options in an almost $r = 0$ world, we set $r = 0$ as in **?**.

Parameters in the SVCJ model can be interpreted as follows. Between the return process (5) and variance process (6), ρ is the correlation between two Brownian motions W_t^s and W_t^v. In the variance process, κ is the speed for conversion to long-term variance, θ is the long-term variance, and σ_v is the volatility of the variance process. The jump components in return and variance precesses has a frequency of jumps of λ as shown in (8). To be positive for the variance process, it has a jump size Z_t^v which is assumed to be exponentially distributed with positive mean μ_v. And, given the jump size of the variance process Z_t^y, the jump size in the return process Z_t^y is assumed to be normally

distributed with mean $\mu_y + \rho_j Z_t^v$ and variance σ_y^2.

The SVCJ includes a rich family of models. If constraints on the parameters of the SVCJ models are imposed, a variety of stochastic volatilities or jump diffusions could be obtained. For example, if we set Z_t^v in (10) as zero, jumps are only present in prices and the model reduces to the SVJ model of **?**; If we set $\lambda = 0$, the model does not exhibit jumps and reduces to the original SV model of **?**; If we set $\kappa = \theta = \sigma_v = 0$ and define $Z_t^v = 0$, the model reduces to the pure jump diffusion of **?**; The pure jump diffusion of **?** reduces to the celebrated BS model (**?**) with $Z_t^y = 0$.

Let $\theta = (\theta_1, \ldots, \theta_p)$ denote the model parameter with size p. Because stochastic volatility is a prominent feature in financial time series data, we focus on the SV, SVJ, and SVCJ models. Specifically, we have $\theta = (\mu,\ \rho,\ \alpha,\ \beta,\ V_0,\ \sigma_v)$ with $p = 6$ for the SV model, $\theta = (\mu, \rho,\ \alpha,\ \beta,\ V_0,\ \sigma_v,\ \lambda,\ \mu_y,\ \sigma_y)$ with $p = 9$ for the SVJ model, and $\theta = (\mu,\ \rho,\ \alpha,\ \beta,\ V_0,\ \sigma_v,\ \lambda,\ \mu_y,\ \rho_j,\ \sigma_y,\ \mu_v)$ with $p = 11$ for the SVCJ model.

3.2 Model calibration and stochastic optimisation

Let $p(\omega, T, K)$ denote the observed market option price, and let $m(\theta; \omega, T, K)$ denote an option price with parameter θ. Following **?**, we calibrate the model parameter by solving the problem:

$$\min \mathcal{L}(\theta) = \sum_i \left\{ p(\omega_i, T_i, K_i) - m(\theta; \omega_i, T_i, K_i) \right\}^2. \tag{11}$$

Thus, model calibration using inverse options is essentially an optimisation.

When there exists no closed-form formula for pricing inverse options under stochastic volatility models, we replace it by Monte Carlo estimate, $\widehat{m}(\theta; \omega_i, T_i, K_i)$. In this case, parameter θ is calibrated by solving

$$\min \widehat{\mathcal{L}}(\theta) = \sum_{i=1}^{M} \left\{ p(\omega_i, T_i, K_i) - \widehat{m}(\theta; \omega_i, T_i, K_i) \right\}^2, \tag{12}$$

where M is the number of inverse options. Thus, the model calibration becomes a stochastic optimisation, because $\widehat{m}(\theta; \omega, T, K)$ is calculated using stochastic simulation method.

However, for stochastic volatility models, there exist no closed-form formulae for pric-

ing inverse options. We must employ Monte Carlo simulation. To simulate a path of the stock price, we use the Euler-Maruyama discretization as follows (**?**). Define $Y_{t+1} = \log(S_{t+1}/S_t)$ as the log-return for $t = 1, \ldots, T$. Let $\alpha = \kappa\theta$ and $\beta = 1 - \kappa$. Then, we have

$$Y_t = r + \sqrt{V_{t-1}}\varepsilon_t^y + Z_t^y J_t, \tag{13}$$

$$V_t = \alpha + \beta V_{t-1} + \sigma_v \sqrt{V_{t-1}}\varepsilon_t^v + Z_t^v J_t, \tag{14}$$

where ε_t^y and ε_t^v are the $N(0,1)$ variables with correlation ρ, J_t is a Bernoulli random variable with $P(J_t = 1) = \lambda$, and jump sizes follow $Z_t^y | Z_t^v \sim N(\mu_y + \rho_j Z_t^v, \sigma_y^2)$ and $Z_t^v \sim Exp(\mu_v)$. Then, the path of asset price under the SVCJ model is obtained through

$$S_t = S_0 \exp^{(Y_1 + \cdots + Y_t)} \text{ for } t = 1, \ldots, T, \tag{15}$$

where S_0 denotes the initial stock price.

Now, we are ready to outline procedures to price inverse options using Monte Carlo simulation. We use N to denote the simulation sample size.

Step 1. Generate the following random variables:

(a) $J_t^{(n)} \sim Ber(\lambda)$,

(b) $Z_t^{v,(n)} \sim Exp(\mu_v)$,

(c) $Z_t^{y,(n)} | Z_t^{v,(n)} \sim N(\mu_y + \rho_j Z_t^v, \sigma_y^2)$,

(d) $\begin{pmatrix} \varepsilon_t^{v,(n)} \\ \varepsilon_t^{y,(n)} \end{pmatrix} \sim N\left(\begin{pmatrix} 0 \\ 0 \end{pmatrix}, \begin{pmatrix} 1 & \rho \\ \rho & 1 \end{pmatrix} \right),$

for $t = 1, \ldots, T$ and $n = 1, \ldots, N$.

Step 2. Calculate $(Y_t^{(n)}, V_t^{(n)})$ using (13) and (14) for $t = 1, \ldots, T$ and $n = 1, \ldots, N$.

Step 3. Calculate $S_t^{(n)}$ using (15) for $t = 1, \ldots, T$ and $n = 1, \ldots, N$.

Step 4. Price the inverse option price using sample mean,

$$\widehat{m}(\theta; \omega, T, K) = \frac{e^{-rT}}{N} \sum_{n=1}^{N} \frac{1}{S_T^{(n)}} \max\left\{\omega(S_T^{(n)} - K),\ 0\right\}.$$

The magnitude of Monte Carlo simulation error in $\widehat{\mathcal{L}}(\theta)$ may dominate the increase in the loss function when updating a parameter. Consequently, the optimisation process is failed. To tackle this problem, we provide an approach with common random numbers for variance reduction (**?**). The idea is to generate one set of random samples and stick to this set of random samples through the whole process of solving stochastic optimisation (12). See also **?**.

To apply common random numbers, one generates samples having the Bernoulli and exponential distributions (**?**). The quantile function for the Bernoulli random variable with parameter λ is $F_B^{-1}(u, \lambda) = I_{\{u>(1-\lambda)\}}(u)$, and the quantile function for the exponential random variable with mean μ is $F_E^{-1}(u, \mu) = -\frac{\log(u)}{\mu_v}$. In addition, we generate the correlated normal random variables $\varepsilon_t^{v,(n)}$ and $\varepsilon_t^{y,(n)}$ from two independent normal random variable through the Cholesky decomposition. Thus, in calculating $\widehat{m}(\theta; \omega, T, K)$, we simply replace Step 1 by Step 1*:

Step 1*. Generate $U_{i,t}^{(n)} \overset{i.i.d.}{\sim} U(0,1)$ for $i = 1, 2$ and $Z_{j,t}^{(n)} \overset{i.i.d.}{\sim} N(0,1)$ for $j = 1, 2, 3$ for $t = 1, \ldots, T$ and $n = 1, \ldots, N$. Then, set

(a) $J_t^{(n)} = I_{\{U_{1,t}^{(n)}>(1-\lambda)\}}\left(U_{1,t}^{(n)}\right)$,

(b) $Z_t^{v,(n)} = -\frac{\log\left(U_{2,t}^{(n)}\right)}{\mu_v}$,

(c) $Z_t^{y,(n)} = (\mu_y + \rho_j Z_t^{v,(n)}) + \sigma_y Z_{1,t}^{(n)}$,

(d) $\varepsilon_t^{v,(n)} = Z_{2,t}^{(n)}$,

(e) $\varepsilon_t^{y,(n)} = \rho Z_{2,t}^{(n)} + \sqrt{1 - \rho^2} Z_{3,t}^{(n)}$,

for $t = 1, \ldots, T$ and $n = 1, \ldots, N$.

3.3 Implied parameters

For each trading day, we include all intraday transaction of inverse options and calibrate a set of model parameter for each day. As a remark, all analysis through out this paper is carried out using Matlab (R2021a) in a desktop (Intel Core i9 CPU with 64 GB RAM). We set $N = 10,000$ as Monte Carlo sample size. To calibrate the BS model, we use the Matlab solver `fminsearch`. To calibrate the SV, SVJ, SVCJ models, we use the Matlab solver `lsqnonlin` for optimisation with Levenberg-Marquardt algorithm and set 'FunctionTolerance' as 10^{-4}. In addition, to ensure the positiveness of the stochastic volatility models, instead of using the Feller condition, $2\kappa\theta > \sigma_v^2$ (or $2\alpha > \sigma_v^2$ by reparametrization), we impose constraints on parameters $\alpha > 0$, $\beta < 1$, $V_0 > 0$. We impose a natural constraint on the correlation coefficient between two Brownian motions, $-1 \leq \rho \leq 1$. For the SVJ and SVCJ models, λ refers to the probability of jump, thus it has to satisfy $0 \leq \lambda \geq 1$. For the SVCJ model, the average jump size for the volatility needs to satisfy $\mu_v \geq 0$.

Figures 9 to 12 provide times series plots for the implied parameters for the BS, SV, SVJ, and SVCJ models, calibrated on a daily basis, respectively. For the BS model, the calibrated parameter σ is volatile across time. For the SV, SVJ, and SVJ models, some implied parameters appear to be constant yet some have huge fluctuations across time.
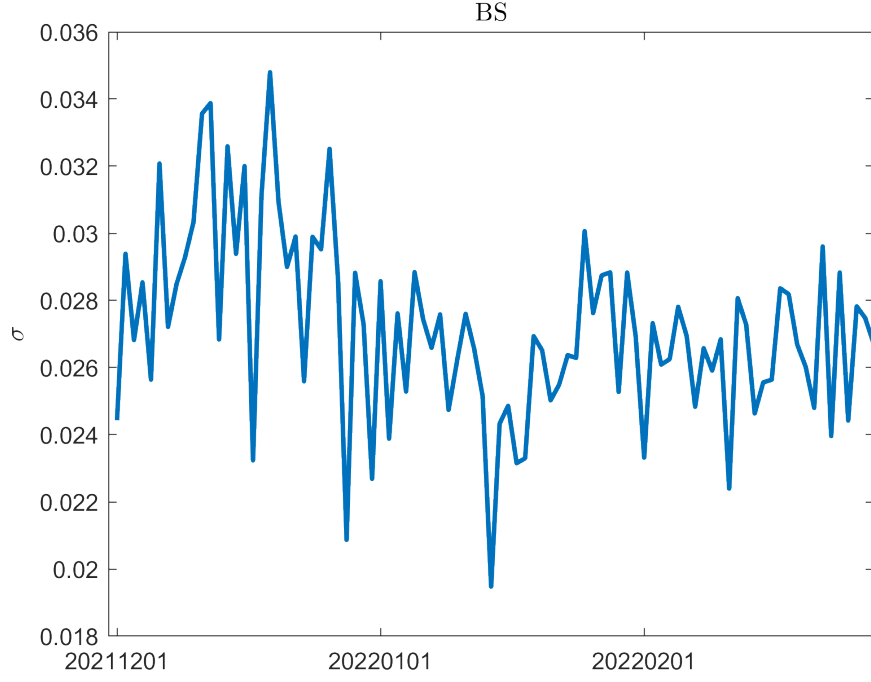
Figure 9: **Implied parameters for the BS model**. This figure provides time series plot for daily calibrated implied parameters for the BS model. Deribit_inverse_BTC_options

Figure 10: **Implied parameters for the SV model**. This figure provides time series plot for daily calibrated implied parameters for the SV model. Deribit_inverse_BTC_options
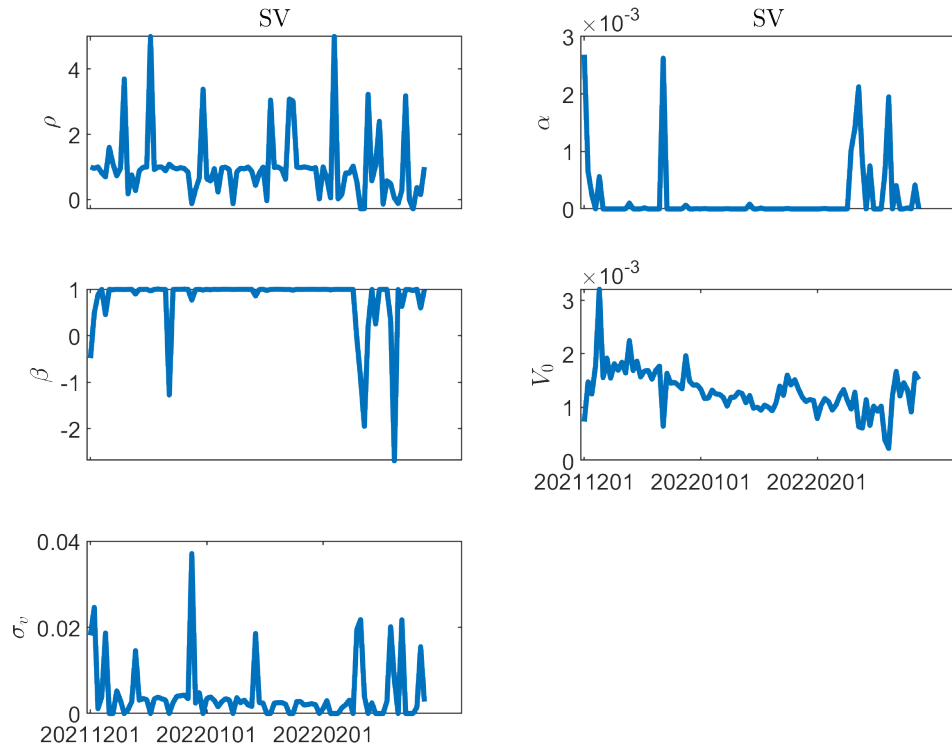
Figure 11: **Implied parameters for the SVJ model**. This figure provides time series plot for daily calibrated implied parameters for the SVJ model.
Deribit_inverse_BTC_options
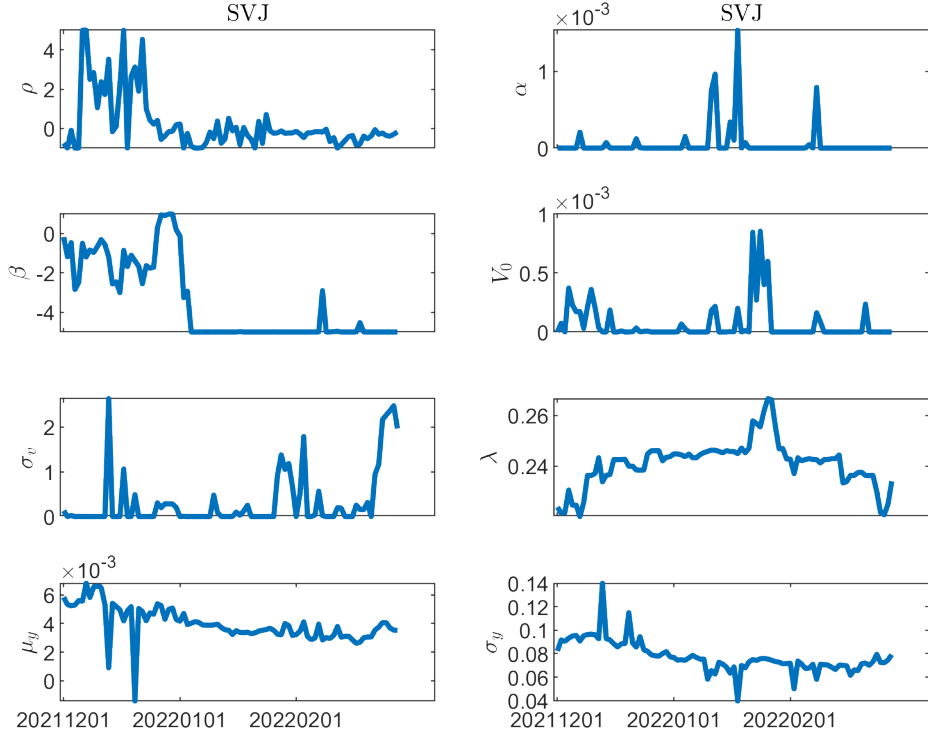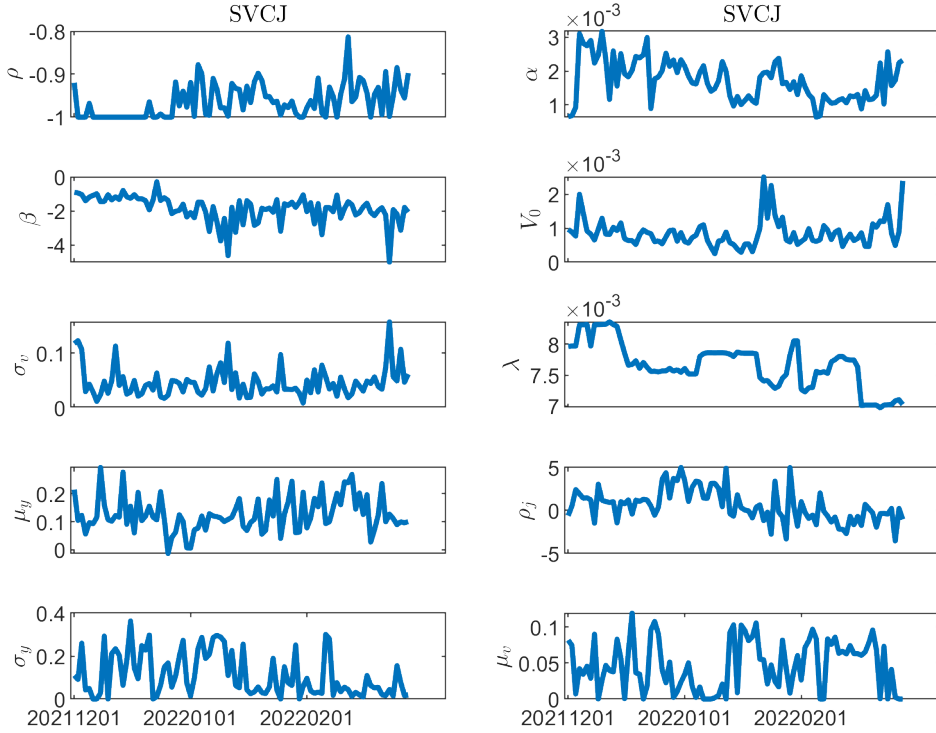

Figure 12: **Implied parameters for the SVCJ model**. This figure provides time series plot for daily calibrated implied parameters for the SVCJ model.
Deribit_inverse_BTC_options

Moreover, suppose the implied parameter is denoted as $\widehat{\theta}$. To measure if the model fits inverse options well, we calculate the in-sample root-mean-squared-error (RMSE) by

$$\text{In-sample RMSE} = \sqrt{\frac{1}{M}\sum_{i=1}^{M}\left\{p(\omega_i, T_i, K_i) - \widehat{m}(\widehat{\theta}; \omega_i, T_i, K_i)\right\}^2}. \tag{16}$$

Figure 13 provides boxplots and time series plots to compare the in-sample RMSE of in-sample fit among these four models. Unlike the fluctuating time series plots for the implied parameters in Figures 9 to 12, the time series plots for the in-sample RMSE among the four models are rather stable. Furthermore, the SVCJ model is dominating because it produces the least in-sample RMSE, followed by the SVJ, SJ, and BS model. Although SVCJ and SVJ models are indistinguishable in most cases, the SVJ model produces extremely high in-sample RMSE at some times. This is possibly because the SVJ model includes simply jump components for the return process, but the SVCJ model includes jumps for both return and volatility processes. Thus, the SVJ model is less stable in fitting model prices than the SVCJ model. The contrast between the volatile implied parameters and stable in-sample RMSE is an numerical evidence that multiple parameters produce the same option prices. This observation is consistent with the addressed statistical difficulties in fitting a stochastic volatility model with option prices as in ? and ?.
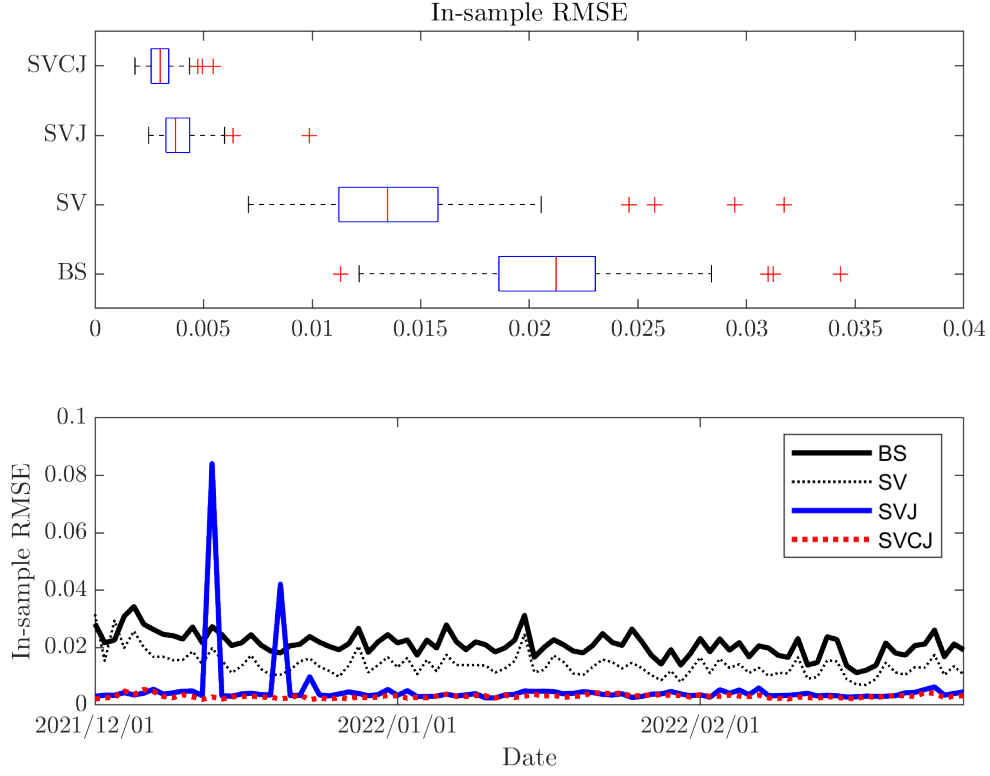
Figure 13: **In-sample root-mean-squared errors**. The upper and lower panels provide boxplots and time-series plots for RMSEs in calibrating intrady inverse option prices under the BS, SV, SVJ, and SVCJ models. The study period spans from December 1, 2021 to February 28, 2022. ⌕ `Deribit_inverse_BTC_options`

Table 4 summarizes the average implied parameters from December 1, 2021 to February 28, 2022. We also convert α and β to κ and θ for better presentations. It is clear that the estimated parameters differ from those obtained in **?**. This is underlined by current empirical findings that historical returns of an underlying and options data yield different parameters. For the BS model, the average implied volatility is 0.0272, which equals 51.97% on a yearly basis. For comparisons, the average implied volatility for options in S&P 500 stocks is about 30%.

In the following, our analysis addresses the issue that multiple combinations of parameters may produce the same price of inverse options. First, we focus on implied parameters for the SV, SVJ, and SVCJ models. Recall that ρ refers to the correlation between the Wiener processes of the return and volatility processes. However, the SV, SVJ, and SVCJ models do not agree the same values for ρ. In fact, the average implied ρ are 0.9798, 0.2001, and -0.9633 for the SV, SVJ, and the SVCJ models, respectively.

Second, θ refers to the value of long term volatility, but it is interesting that these three models do not agree in the value of θ: the average implied θ are 0.0010, 0.0000, and 0.0006 for the SV, SVJ, and SVCJ models. On the other hand, the value of θ can be compromised by the value of σ_v, which refers to the volatility of the volatility process: The higher θ is, the lower σ_v is. The SV, SVJ, and SVCJ models yield the average values of σ_v at 0.0043, 0.3301, 0.0469, respectively.

Between the SVJ and SVCJ models, recall that λ refers to the frequency of jump. There is a trade-off between the value of θ and λ. The average values of λ are 0.2410 and 0.0077 for the SVJ and SVCJ models, respectively. Compared with the SVJ model, the SVCJ has higher long-term probability, but it has lower jump frequency. Next, recall that μ_y refers to the average jump size of the return process. And there is also a trade-off between the value of λ and μ_y. The average values of the μ_y are 0.0040 and 0.1272 for the SVJ and SVCJ models, respectively. Compared with the SVJ model, the SVCJ model has higher frequency of jumps, but has smaller average jump size.

Table 4: **Average implied parameters**. This table reports average implied parameters for the BS, SV, SVJ, and SVCJ models using intraday inverse options calibrated on a daily basis. The study period spans from December 1, 2021 to February 28, 2022. **Q** `Deribit_inverse_BTC_options`

	BS	SV	SVJ	SVCJ
σ	0.0272			
ρ		0.9798	0.2001	-0.9633
α		0.0002	0.0001	0.0017
β		0.7982	-3.5021	-1.8620
V_0		0.0013	0.0001	0.0009
σ_v		0.0043	0.3301	0.0469
λ			0.2410	0.0077
μ_y			0.0040	0.1272
ρ_j				0.5722
σ_y			0.0774	0.1109
μ_v				0.0465
Reparametrisation				
κ		0.2018	4.5021	2.8620
θ		0.0010	0.0000	0.0006

To investigate if the SVCJ model suffers an overfitting problem, we calculate the out-of-sample RMSE at day t by replacing the parameters implied from day t to those implied from day $(t-1)$ in (16). We provide boxplots and time series plots for the out-of-sample RMSE in Figure 14, and find the SVCJ remains dominating and is followed by the SVJ, SV, and BS model.
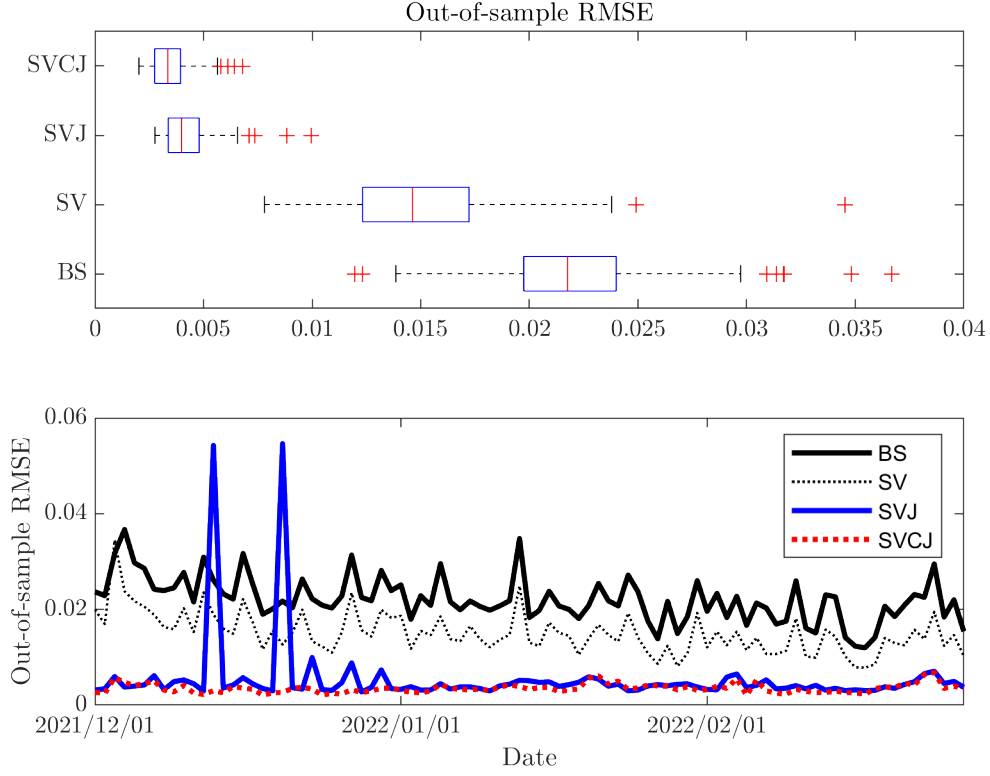
Figure 14: **Out-of-sample root-mean-squared errors**. The upper and lower panels provide boxplots and time-series plots for RMSEs in calibrating intrady inverse option prices under the BS, SV, SVJ, and SVCJ models. The study period spans from December 1, 2021 to February 28, 2022. ⚲ `Deribit_inverse_BTC_options`

4 Dynamic delta hedging

In this section, Section 4.1 provides a general Delta formula that is applicable under complex dynamics. With this Delta formula, we implement dynamic delta hedging using inverse options and compare whether the SVCJ model outperforms its nested ones in Section 4.2.

4.1 The Delta formula

The Delta is price sensitivity with respect to the initial underlying price, specifically,

$$\Delta = \frac{\partial}{\partial S_0} m(S_0, \omega, K, T, \theta),$$

where $m(S_0, \omega, K, T, \theta)$ follows the notations introduced before. When a closed-form formula of an option price exists, the Delta can be calculated by direct differentiation. For example, under the BS model, **?** provide the Delta formula

$$\omega e^{\sigma^2 T} S^{-2} K \Phi(\omega d_3). \tag{17}$$

However, the calculate of Delta under a more complicated model is challenging and has to be calculated with more sophisticated numerical procedures.

In the following, we apply the *parameter derivative* in **?** to provide the Delta formula for the inverse option. As an extension to **?**, the parameter derivative approach is generally applicable and simple to implement. Specifically, it allows us to provide a formula to calculate an unbiased Delta, as long as the stock prices at maturity can be generated as a function of S_0 and a random vector χ, i.e., $S_T = S_0 g(\chi)$. Let I_A denote the indicator function for set A. Then, we rewrite the payoff function of the inverse option as a product of smooth function and an indicator function,

$$
\begin{aligned}
\wp_{inverse}(\omega, K, T) &= S_T^{-1} \max\{\omega(S_T - K), 0\} \\
&= S_T^{-1}\omega(S_T - K)I_{\{\omega(S_T - K)>0\}} \\
&= \omega\left(1 - \frac{1}{S_0}\frac{K}{g(\chi)}\right) I_{\{\omega(S_T - K)>0\}}.
\end{aligned}
$$

With the parameter derivative, we obtain the Delta formula:

$$
\begin{aligned}
\Delta &= e^{-rT}\mathsf{E}\left\{\frac{\partial \wp_{inverse}(\omega, K, T)}{\partial S_0}\right\} \\
&= e^{-rT}\mathsf{E}\left\{\omega\left(\frac{1}{S_0^2}\frac{K}{g(\chi)}\right) I_{\{\omega(S_T - K)>0\}}\right\} \\
&= e^{-rT}\mathsf{E}\left\{\omega\left(\frac{1}{S_0}\frac{K}{S_T}\right) I_{\{\omega(S_T - K)>0\}}\right\}. \tag{18}
\end{aligned}
$$

As a note, the form of the Delta formula is the same under the BS, SV, SVJ, and SVCJ models, but the differences come from how S_T is generated. Under the BS model, when the expectation is carried out through standard calculus, (18) reduces to (17).

For the inverse BTC call option, the Delta can be approximated by

$$
\begin{aligned}
\Delta &= \mathrm{e}^{-rT}\mathsf{E}\left\{\left(\frac{1}{S_0}\frac{K}{S_T}\right)I_{\{(S_T-K)>0\}}\right\} = \mathrm{e}^{-rT}\frac{K}{S_0}\mathsf{E}\left\{\frac{1}{S_T}I_{\{(S_T-K)>0\}}\right\} \\
&\approx \mathrm{e}^{-rT}\frac{K}{S_0}\frac{1}{S_0}Pr\left\{(S_T-K)>0\right\} \\
&\leq \mathrm{e}^{-rT}\frac{K}{S_0}\frac{1}{S_0},
\end{aligned}
\tag{19}
$$

where $Pr(E)$ denotes the probability that an event E occurs. Because S_0 is the value of a BTC denominated in USD, which has the average price of 43,875.72 USD during the study period, thus Delta is positive but less than about $\frac{1}{43,375.72} = 2.3 \times 10^{-5}$. This is an extremely small value. Similarly, the inverse BTC put option has an approximate Delta:

$$
\begin{aligned}
\Delta &\approx -\mathrm{e}^{-rT}\frac{K}{S_0}\frac{1}{S_0}Pr\left\{(S_T-K)<0\right\} \\
&\geq -\mathrm{e}^{-rT}\frac{K}{S_0}\frac{1}{S_0}.
\end{aligned}
\tag{20}
$$

Thus, an inverse BTC put option has negative Delta but its absolute value is of the scale of 10^{-5}.

Figure 15 depicts Deltas under the BS, SV, SVJ, and SVCJ models for different time to maturity. Each panel presents Deltas with $T = 7$ (one week), $T = 28$ (four weeks), $T = 90$ (a quarter), and $T = 180$ (half year), respectively. We use implied parameters calibrated on January 1, 2022 as the parameter for each model. In addition, we set $S_0 = 47128.85$, which is the last price of BTC on January 1, 2022. The Delta under the SV, SVJ, and SVCJ models are calculated using Monte Carlo simulation with a sample size of $N = 10,000$. We overlay a horizontal line in each panel. Recall the Delta formula (18):

$$
\Delta = \mathrm{e}^{-rT}\mathsf{E}\left\{\omega\left(\frac{1}{S_0}\frac{K}{S_T}\right)I_{\{\omega(S_T-K)>0\}}\right\} = \omega\mathrm{e}^{-rT}\mathsf{E}\left\{\left(\frac{1}{S_0}\frac{K}{S_T}\right)I_{\{\omega(S_T-K)>0\}}\right\}.
\tag{21}
$$

Because the expectation in the right-hand side of (21) is positive (assuming BTC would never has a negative price), the sign of inverse BTC call and put options depend on ω.

Thus, inverse BTC call and put options have positive and negative Deltas, respectively.

First, Deltas are of extremely small values at a magnitude of 10^{-5}. This observation is consistent with our approximations in (19) and (20). Second, for short-term and mid-term inverse options, i.e., $T = 7$ and $T = 28$, Deltas under the four models are extremely close. For long-term options, i.e., $T = 90$ and $T = 180$, Deltas under different models deviate. However, BS and SV models produce close Deltas, and also the SVJ and SVCJ models produce almost identical Deltas.
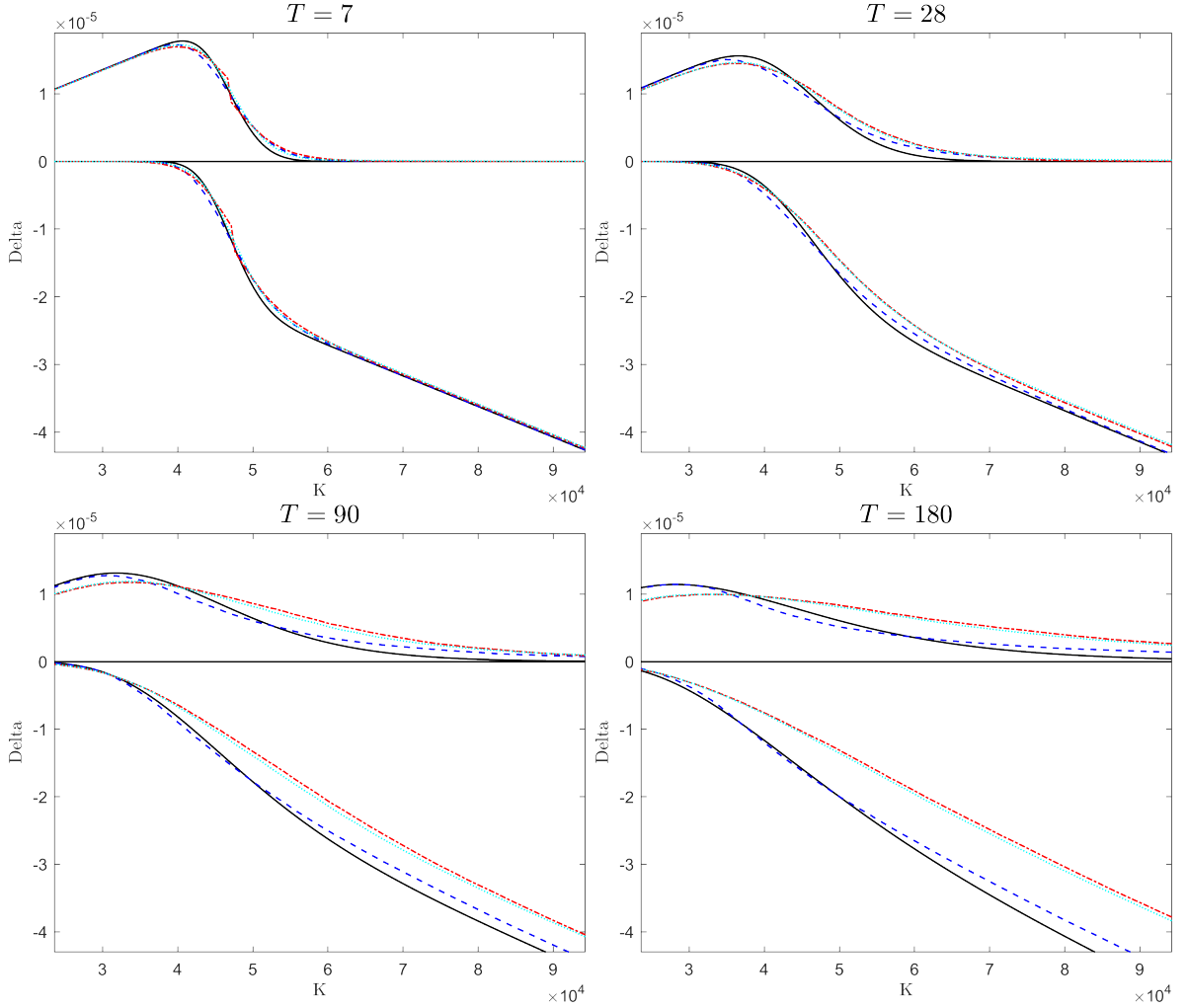

Figure 15: **Deltas under the BS, SV, SVJ, and SVCJ models**. Each panel presents Deltas with different time to maturity: $T = 7$ (one week), $T = 28$ (four weeks), $T = 90$ (a quarter), and $T = 180$ (half year). We overlay a horizontal line in each panel. Lines above and below the horizontal line are Deltas for inverse BTC call and put options, respectively. The Delta under the BS model is in a black-solid line, the Delta under the SV model is in a orange dashed line, the Delta under the SVJ model is in a red dashed-dotted line, and the Delta under the SVCJ model is in a cyan dotted line. **Q** Deribit_inverse_BTC_options

4.2 Hedging performance

Now, we describe how to implement the dynamic Delta hedging for inverse options. Suppose we are hedging on a daily basis, $t = 1, \ldots, T$. Given an option contract, let $P(t)$ denote its price denoted in BTC at time t. Let $\Delta(t)$ denote the Delta of this option at time t. Consider a Delta-neutral portfolio which is composed of three ingredients:

1. A short position in an inverse option of value $P(t)$

2. A long position of $\Delta(t)$ number of BTC

3. An amount $B(t)$ in the money market denoted in USD

To start, the Delta-neutral portfolio has value denoted in USD:

$$\Pi(1) = -P(1)S(1) + \Delta(1)S(1) + B(1), \tag{22}$$

where we set

$$B(1) = P(1)S(1) - \Delta(1)S(1)$$

to form a self-rebalancing portfolio with zero initial value. Then, the dynamic hedge procedures are repeated on a daily basis as follows. At day t, we adjust the position of BTC from $\Delta(t-1)$ to $\Delta(t)$ and obtain

$$\Pi(t) = -P(t)S(t) + \Delta(t)S(t) + B(t),$$

where value changes in BTC is added to the money market account,

$$B(t) = e^{r(t-(t-1))}B(t-1) - S(t)(\Delta(t) - \Delta(t-1)).$$

Repeat the above procedures until the time to maturity T. The hedging portfolio value at maturity is $\Pi(T)$. To measure the performance of hedging, we define the relative hedging error, denoted by π, as

$$\pi = \frac{e^{-rT}\Pi(T)}{P(1)S(1)}.$$

To fully explore dynamic Delta hedging under various models with intraday transaction, we avoid creating non-existing prices which are not traded. As a result, we rearrange the data as follows. We pick up the last traded inverse options for each trading day, then, fixing a trading day in the study period and a maturity-strike combination, we check if this inverse option has consecutive trades to maturity. If this is the case, we record this inverse option and implement dynamic delta hedging. Otherwise, we simply ignore it. We repeat the above procedure for each trading during the study period, and we calculate the relative hedging errors at various maturity-money categories at each trading day in the study period.

Figure 16 summarizes the relative hedging error for inverse BTC call options with boxplots across nine maturity-moneyness categories. First, deep OTM inverse BTC call options do not have consecutive trades to maturity during our study period. As result, panels for deep OTM inverse BTC call options are empty. However, for other maturity-moneyness categories, the distributions of relative hedging errors among the BS, SV, SVJ, and SVCJ model are indistinguishable. The same phenomena for inverse BTC put options are observed in Figure 17: Distributions of relative hedging errors with dynamic Delta hedging for inverse BTC put options under the BS, SV, SVJ, and SVCJ models, are indistinguishable. Panels for deep OTM inverse put options are empty.

The empirical results that dynamic Delta hedging for inverse options with a more complicated model does not necessarily outperform that with the simple BS model. These results are in fact consistent with existing literature for vanilla options **?**. The prediction error caused by a model is one reason why hedging becomes indistinguishable across models. In the case of inverse options, as shown in Section 4.1, Deltas for short-term and mid-term options are extremely close. In fact, according to Table 1, about 80% inverse options are short-term or mid-term. Thus, the majority inverse options actually use indistinguishable Deltas across models in dynamic Delta hedging. Thus, we observe indistinguishable relative hedging errors.
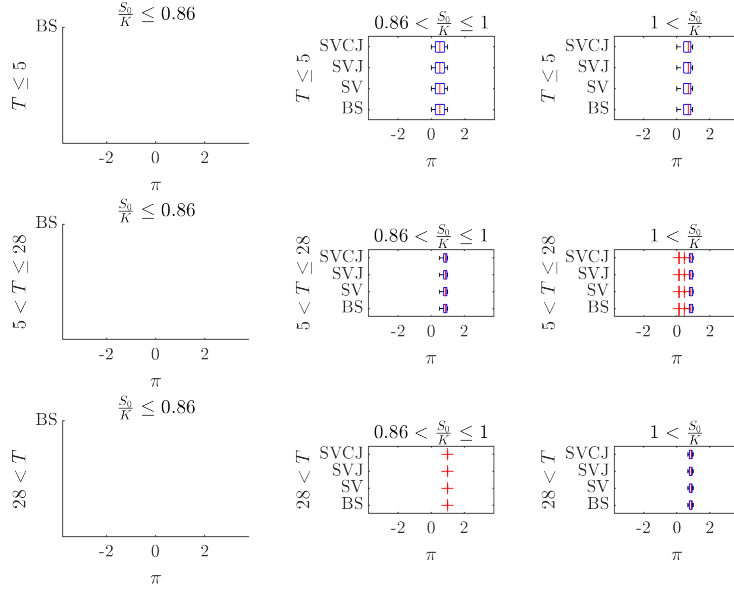
Figure 16: **Relative hedging errors for inverse BTC call options**. This figure compares boxplots of relative hedging errors for inverse BTC put options at each maturity-monyeness cateogory. Panels for deep OTM inverse call options are empty, because there are no consecutively traded put options. The study period spans from December 1, 2021 to February 28, 2022. **Q.** `Deribit_inverse_BTC_options`

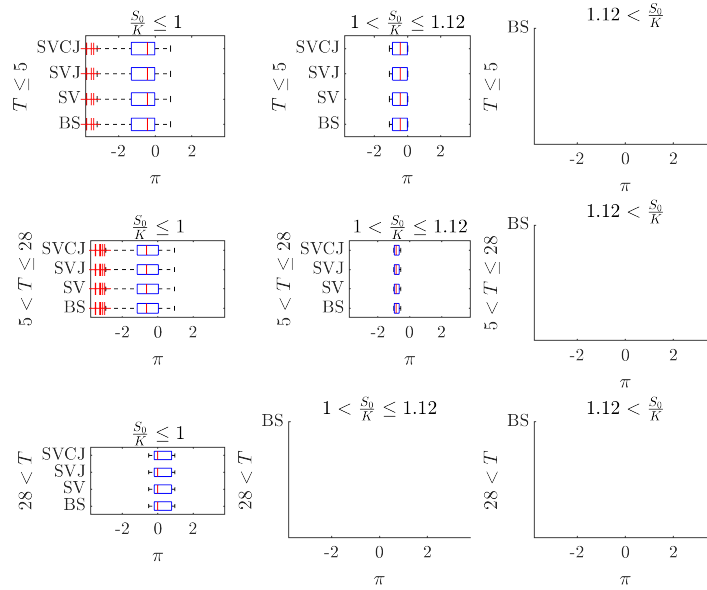Figure 17: **Relative hedging errors for inverse BTC put options**. This figure compares boxplots of relative hedging errors for inverse BTC put options at each maturity-monyeness cateogory. Panels for deep OTM inverse put options are empty, because there are no consecutively traded put options. The study period spans from December 1, 2021 to February 28, 2022. **Q.** `Deribit_inverse_BTC_options`

5 Conclusion

In this paper, we analyse intraday transaction of inverse BTC optoins traded in Deribit. We first summarize stylized features of inverse options and find a puzzle of implied volatility slippery in inverse options. Then, we consider complex models including stochastic volatility and jumps. We provide a feasible simulation scheme for model calibration. Our empirical analysis finds that the SVCJ model out-performs its nested models in terms of in-sample and out-of-sample pricing analysis. Furthermore, we provide the Delta formula of the inverse option under complex models. The Delta formula allows us to implement the dynamic hedging routines. In dynamic Delta hedging, the SVCJ model is indistinguishable to simpler models in terms of relative hedging errors.

Understanding the cropto currencies and its derivatives is of considerable importance. Along this line of research, portfolio management, trading, and investor's behaviour, deserve further research. It is also worthy of exploring arbitrage opportunity from the implied volatility slippery and investigating put-call parity for the inverse option. On the other hand, it is found that multiple parameters may produce the same prices for inverse options. Thus, it would be interesting to see if the parameter from historical data could be incorporated when calibrating a model. Second, fast and accurate pricing for inverse options and higher-order Greeks requires further attention.

References

Alexander, C., J. Deng, J. Feng, and H. Wan (2022). Net buying pressure and the information in bitcoin option trades. *Journal of Financial Markets*.

Alexander, C. and A. Imeraj (2021). Inverse options in a Black-Scholes world. Available at arXiv: https://arxiv.org/abs/2107.12041.

Alexander, C. and A. Imeraj (2022). Delta hedging bitcoin options with a smile. Available at SSRN: https://ssrn.com/abstract=4097909.

Bakshi, G., C. Cao, and Z. Chen (1997). Empirical performance of alternative option pricing models. *The Journal of Finance 52*(5), 2003–2049.

Bates, D. S. (1996). Jumps and stochastic volatility: Exchange rate processes implicit in deutsche mark options. *The Review of Financial Studies 9*(1), 69–107.

Belaygoro, A. (2005). Solving continuous time affine jump-diffusion models for econometric inference. Available at `https://citeseerx.ist.psu.edu/viewdoc/download?doi=10.1.1.475.9517&rep=rep1&type=pdf`.

Black, F. and M. Scholes (1973). The pricing of options and corporate liabilities. *Journal of Political Economy 81*(3), 637–654.

Cao, M. and B. Celik (2021). Valuation of bitcoin options. *Journal of Futures Markets 41*(7), 1007–1026.

Chen, K.-S. and Y.-C. Huang (2021). Detecting jump risk and jump-diffusion model for bitcoin options pricing and hedging. *Mathematics 9*(20), 2567.

Cont, R. and P. Tankov (2004). Nonparametric calibration of jump-diffusion option pricing models. *The Journal of Computational Finance 7*, 1–49.

Cretarola, A., G. Figà-Talamanca, and M. Patacca (2020). Market attention and bitcoin price modeling: Theory, estimation and option pricing. *Decisions in Economics and Finance 43*(1), 187–228.

Cui, Y., S. del Bano Rollin, and G. Germano (2017). Full and fast calibration of the heston stochastic volatility model. *European Journal of Operational Research 263*(2), 625–638.

Glasserman, P. (2004). *Monte Carlo Methods in Financial Engineering*. New York: Springer.

Hacioglu, U. (2019). *Blockchain economics and financial market innovation: Financial innovations in the digital age*. Switzerland: Springer.

Härdle, W. K., C. R. Harvey, and R. C. Reule (2020). Understanding cryptocurrencies. *Journal of Financial Econometrics 18*(2), 181–208.

He, C., J. S. Kennedy, T. F. Coleman, P. A. Forsyth, Y. Li, and K. R. Vetzal (2006). Calibration and hedging under jump diffusion. *Review of Derivatives Research 9*(1), 1–35.

Heston, S. L. (1993). A closed-form solution for options with stochastic volatility with applications to bond and currency options. *The Review of Financial Studies 6*(2), 327–343.

Hou, A. J., W. Wang, C. Y. Chen, and W. K. Härdle (2020). Pricing cryptocurrency options. *Journal of Financial Econometrics 18*(2), 250–279.

Hu, Y., S. T. Rachev, and F. J. Fabozzi (2019). Modelling crypto asset price dynamics, optimal crypto portfolio, and crypto option valuation. Available at arXiv: https://arxiv.org/abs/1908.05419.

Hull, J. (2014). *Options, Futures, and Other Derivatives* (9 ed.). New York: Prentice Hall.

Jalan, A., R. Matkovskyy, and S. Aziz (2021). The bitcoin options market: A first look at pricing and risk. *Applied Economics 53*(17), 2026–2041.

Li, L., A. Arab, J. Liu, J. Liu, and Z. Han (2019). Bitcoin options pricing using LSTM-based prediction model and blockchain statistics. In *2019 IEEE international conference on Blockchain (Blockchain)*, pp. 67–74. IEEE.

Lyuu, Y.-D. and H.-W. Teng (2011). Unbiased and efficient Greeks of financial options. *Finance and Stochastics 15*(1), 141–181.

Lyuu, Y.-D., H.-W. Teng, Y.-T. Tseng, and S.-X. Wang (2019). A systematic and efficient simulation scheme for the Greeks of financial derivatives. *Quantitative Finance 19*(7), 1199–1219.

Madan, D. B., S. Reyners, and W. Schoutens (2019). Advanced model calibration on bitcoin options. *Digital Finance 1*(1), 117–137.

Matic, J. L., N. Packham, and W. K. Härdle (2021). Hedging cryptocurrency options. Revised and resubmitted to *Review of Derivatives Research*. Available at arXiv: https://arxiv.org/abs/2112.06807.

Merton, R. C. (1976). Option pricing when underlying stock returns are discontinuous. *Journal of Financial Economics 3*(1-2), 125–144.

Mrázek, M., J. Pospíšil, and T. Sobotka (2016). On calibration of stochastic and fractional stochastic volatility models. *European Journal of Operational Research 254*(3), 1036–1046.

Nakamoto, S. (2008). Bitcoin: A peer-to-peer electronic cash system. *Decentralized Business Review*, 21260.

Ross, S. M. (2022). *Simulation* (6 ed.). London, UK: Academic Press.

Saef, D., O. Nagy, S. Sizov, and W. K. Härdle (2021). Understanding jumps in high frequency digital asset markets.

Scaillet, O., A. Treccani, and C. Trevisan (2020). High-frequency jump analysis of the bitcoin market. *Journal of Financial Econometrics 18*(2), 209–232.

Siu, T. K. and R. J. Elliot (2021). Bitcoin option pricing with a SETAR-GARCH model. *The European Journal of Finance 27*(6), 564–595.

Teng, H.-W. (2022). Importance sampling for calculating the value-at-risk and expected shortfall of the quadratic portfolio with t-distributed risk factors. *Computational Economics*.

Zulfiqar, N. and S. Gulzar (2021). Implied volatility estimation of bitcoin options and the stylized facts of option pricing. *Financial Innovation 7*(1), 1–30.

Appendix

Table 5: **Data descriptions**. This table lists columns and their descriptions for the intra-day transaction of Deribit inverse options through the Blockchain-Research-Center.com.

Index	Column	Type	Description
1	q	number	Quantity
2	p	number	Option price denoted in BTC
3	s	string	
4	t	integer	Timestamp (13 digit UNIX format, milliseconds since the UNIX epoch)
5	d	string	Date (YYYY/mm/dd)
6	$trade\_seq$	integer	The sequence number of the trade within instrument
7	$trade\_id$	string	Unique (per currency) trade identifier
8	$tick\_direction$	integer	Direction of the "tick" (0=Plus Tick, 1 = Zero-Plus Tick, 2 =Minus Tick, 3 = Zero-Minus Tick)
9	iv	number	implied volatility
10	$instrument\_name$	string	UNDERLYING-MATURITY-STRIKE(Call/Put)
11	$index\_price$	number	the price of the underyling BTC denoted in USD
12	$direction$	string	